Chinese Physics C

Nuclear data for the cyclotron production of ^{117}Sb and ^{90}Nb

Enferadi Milad[1]   Sadeghi Mahdi[2;1)]

[1] Islamic Azad University, Science and Research Branch, Tehran, Iran

[2] Agricultural, Medical and Industrial Research School, Nuclear Science and Technology Research Institute, P.O. Box: 31485/498, Karaj, Iran

Abstract: This presented study is to make comparison of cross sections to produce ^{117}Sb and ^{90}Nb via different reactions with particle incident energy up to 70 MeV as a part of systematic studies on particle-induced activations on enriched Sn, Y_2O_3 and ZrO_2 targets, theoretical calculation of production yield, calculation of required thickness of target and suggestion of optimum reaction to produce Antimony-117 and Niobium-90.

Key words: ^{117}Sb, ^{90}Nb, excitation functions, TALYS-1.2, ALICE/ASH

PACS: 29.85.-c   **DOI:** 10.1088/1674-1137/35/3/007

1 Introduction

^{117}Sb ($T_{1/2}$=2.8 h) decays mainly by EC (only 1.7% β^+) with the emission of the nearly single X-ray of 158.56 keV suitable for imaging. In fact, the energies and intensities of the emitted photons in ^{117}Sb decay are very similar to the photons emitted by the widely used SPECT isotope ^{123}I. Internal dosimetry constitutes a very important part of radionuclide therapy but because of the absence of penetrating photon emission, ^{117}Sb can be produced and used for labeling a precursor using the same technique as for ^{119}Sb. Both isotopes being of the same element also ensures identical properties in-vivo. In this respect, the isotope pair ^{117}Sb/^{119}Sb resembles the ^{86}Y/^{90}Y pair [1, 2]. The radioisotope ^{117}Sb can give SPECT or SPECT/CT based patient-specific 3D dosimetry. From the planar scintigraphy and the transversal slice through the SPECT tomography of the Jaszczak Phantom, it can be seen that^{117}Sb is a suitable imaging isotope [2, 3].

Auger electron emitting radionuclides have potential for the therapy of small-size cancers because of their high level of cytotoxicity, low-energy, high linear energy transfer, and short range biologic effectiveness [2–7]. Besides the direct effect of Auger electrons on DNA double strands, an indirect radiation effect of Auger energy deposition will occur via production of radicals. The radicals diffuse freely in the intracellular space and can cause further DNA damage [4–7]. ^{64}Cu combines both β^+ and Auger electron emissions in its decay mode, hence considered as promising radionuclide targeting DNA. Similarly, ^{90}Nb ($T_{1/2}$=14.6 h) combines positron and Auger electrons with favorable energy and intensity (2.02 keV, 77.7% and 13.4 keV, 17.5%), and therefore it is a potential candidate radionuclide for targeted radionuclide therapy. Apart from probable clinical applications, ^{90}Nb may also find its utility in simulating the behavior of ^{91}Nb ($T_{1/2}$=680 a), a potentially hazardous radionuclide in nuclear waste. In all these applications, ^{90}Nb is preferred in its no-carrier-added state [8, 9].

^{117}Sb and ^{90}Nb excitation functions via ^{117}Sn(p, n)^{117}Sb, ^{118}Sn(p,2n)^{117}Sb, ^{119}Sn(p,3n)^{117}Sb, ^{120}Sn(p, 4n)^{117}Sb, ^{117}Sn(d,2n)^{117}Sb, ^{115}Sn(α,2n)^{117}Te→ ^{117}Sb, ^{90}Zr(p,n)^{90}Nb, ^{91}Zr(p,2n)^{90}Nb, ^{92}Zr(p,3n)^{90}Nb and ^{89}Y(α,3n)^{90}Nb reactions were calculated by AL-ICE/91, ALICE/ASH and TALYS-1.2 codes and compared to existing data. Requisite thicknesses of targets were obtained by SRIM (the Stopping and Range of Ions in Matter) code for each reaction.

2 Methods

2.1 Calculation of excitation function

Nuclear data play a very important role in the

choice of a radioisotope for a medical application. Nuclear structure and the decay data determine the suitability of a radioisotope for diagnostic application while the nuclear reaction data study the possibility of its production in a pure form. The production of non-conventional radionuclides, however, demands detailed nuclear data work covering both experimental investigations and nuclear model calculations. Radioisotopes produced by charged-particle nuclear reactions find important applications in medicine [10, 11]. Nuclear reaction models are frequently needed to provide estimates of the particle-induced reaction cross sections, especially if the experimental data are not available or unable to measure the cross-sections due to the experimental difficulty. Therefore, nuclear reaction model calculations play an important role in the nuclear data evaluation. Besides, these obtained data are necessary to develop more nuclear theoretical calculation models in order to explain nuclear reaction mechanisms and the properties of the excited states in different energy ranges.

The excitation functions of $^{117-120}$Sn, $^{90-92}$Zr+xp, ^{115}Sn, ^{89}Y+α, and ^{117}Sn+xd reactions were calculated by using ALICE/91, ALICE/ASH (GDH Model & Hybrid Model) and TALYS-1.2 codes [12–15]. The codes were used simultaneously to increase the accuracy of calculations. An optimum energy range was determined and employed to avoid the formation of the radionuclide impurities and decrease the excitation functions of the inactive impurities as far as possible. To further achieve the aim, the feasibility of ^{117}Sb and ^{90}Nb production via various nuclear reactions per low/medium energy accelerators was investigated.

2.2   The ALICE/ASH code and Calculation methods of hybrid and geometry-dependent hybrid Models

The ALICE/ASH code [13] is a modified and advanced version of the ALICE code [12]. The geometry dependent hybrid model (GDH) is used for the description of the pre-equilibrium particle emission. Intranuclear transition rates are calculated using the effective cross section of nucleon-nucleon interactions in nuclear matter. Corrections are made to the GDH model for the treatment of effects in peripheral nuclear regions. The number of neutrons and protons for initial exciton state is calculated using realistic nucleon-nucleon interaction cross sections in nucleus [13]. The exciton coalescence model [16] and the knock-out model are used for the description of the pre-equilibrium complex particle emission. The

equilibrium emission of particles is described by the Weisskopf-Ewing model without detail consideration of angular momentum.

The hybrid model for pre-compound decay is formulated by Blann and Vonach (1983) [17] as

$$\frac{d\sigma_\upsilon(\varepsilon)}{d\varepsilon} = \sigma_R P_\upsilon(\varepsilon),$$

$$P_\upsilon(\varepsilon)d\varepsilon = \sum_{\substack{n=n_0 \\ \Delta n=+2}}^{\overline{n}} [_n\chi_\upsilon N_n(\varepsilon,U)/N_n(E)]g\,d\varepsilon$$
$$\times \left[\frac{\lambda_c(\varepsilon)}{\lambda_c(\varepsilon)+\lambda_+(\varepsilon)}\right]D_n, \qquad (1)$$

Where σ_R is the reaction cross section, $_n\chi_\upsilon$ is the number of particle type υ (proton or neutron) in n exciton hierarchy, $P_\upsilon (\varepsilon)d\varepsilon$ represents number of particles of the υ (neutron or proton) emitted into the unbound continuum with channel energy between ε and ε+dε. The quantity in the first set of square brackets of Eq. (1) represents the number of particles to be found (per MeV) at a given energy ε for all scattering processes leading to one exciton configuration. $\lambda_c(\varepsilon)$ is the emission rate of a particle into the continuum with channel energy ε and, $\lambda_+(\varepsilon)$ is the intranuclear transition rate of a particle. It has been demonstrated that the nucleon-nucleon scattering energy partition function $N_n(E)$ is identical to the exciton state density $\rho_n(E)$, and may be derived by certain conditions on nucleon-nucleon scattering cross sections. The second set of square brackets in Eq. (1) represents the fraction of the υ type particles at an energy which should undergo emission into the continuum, rather than making an intranuclear transition. D_n represents the average fraction of the initial population surviving to the exciton number being treated. The intranuclear cascade calculation results indicated that the exciton model deficiency resulted from a failure to properly reproduce enhanced emission from the nuclear surface [17]. In order to provide a first-order correction for this deficiency the hybrid model was reformulated by Blann and Vonach (1983). In this way the diffuse surface properties sampled by the higher impact parameters were crudely incorporated into the pre-compound decay formalism, in the geometry-dependent hybrid model (GDH). The differential emission spectrum is given in the GDH as

$$\frac{d\sigma_\upsilon(\varepsilon)}{d\varepsilon} = \pi\lambda^2 \sum_{l=0}^{\infty}(2\lambda+1)T_\lambda P_\upsilon(\lambda,\varepsilon), \qquad (2)$$

where λ, is the reduced de Broglie wavelength of the projectile and T_λ represents transmission coefficient for the λth partial wave. Using the total pre-

compound neutron emission spectrum $\frac{\mathrm{d}\sigma_n(\varepsilon)}{\mathrm{d}\varepsilon}$, the cross section which could be involved in the emission of two neutrons is calculated as

$$\sigma_{2n} = \int_{U=0}^{E-B_{2n}} (\mathrm{d}\sigma_n(\varepsilon)/\mathrm{d}\varepsilon)\mathrm{d}\varepsilon, \qquad (3)$$

where B_{2n} represents the sum of the first and the second neutron binding energies. The geometry-dependent influences are manifested in two distinct manners in the formulation of the GDH model. The more obvious is the longer mean free path predicted for nucleons in the diffuse surface region. The second effect is less physically secure, yet seems to be important in reproducing experimental spectral shapes [18, 19].

2.3　The TALYS 1.2 code

The calculational code TALYS can describe nuclear reactions induced by almost all the possible incident particles in the 1 keV–200 MeV energy range [14]. It is equipped with the ECIS–06 code [20] for optical model and direct reaction calculations. The optical model potentials (OMPs) from the compilation of Koning and Delaroche (2003) [21] are the default options for the protons and neutrons. The OMPs for the deuterons, tritons, ^{3}He and α-particles are generated by applying the so-called folding approach [22]. The Reference Input Parameter Library (RIPL) of the IAEA [23] mostly constitutes the TALYS database. The statistical treatment of the compound nucleus is based on the Hauser–Feshbach model along with the width fluctuation correction model of Moldaue (1980) [24]. The pre-equilibrium contribution is estimated by the exciton model [25].

For pre-equilibrium reactions involving deuterons, tritons, Helium-3 and α-particles, a contribution from the exciton model is automatically calculated. In addition to exciton model, the TALYS includes an extension to take into account the direct interactions like stripping, pick-up, break-up and knock-out. These are based on a phenomenological contribution model developed by Kalbach (2005) [26]. The pre-equilibrium cross section is thus given by the sum of an exciton model, nucleon transfer, and knock-out contribution. In the case of loosely bound projectiles (d, ^{3}He, etc.), the break-up channel may play an important role. Therefore, for deuterons a simple model by Kalbach has been included. This leads to an extra contribution in the (d,n) and (d,p) channels. The back-shifted Fermi gas model [27] was selected for level densities. The discrete level schemes of important nuclei in each reaction were properly adjusted for better description of the lower energy region. The γ-ray strength function could be adjusted by the G_{norm} parameter, which acts as a multiplication factor for γ-ray transmission coefficients [28].

2.4　Calculation of the required thickness of target

According to the SRIM code, the required thickness of target was calculated [29]. The physical thickness of the target layer is chosen in such a way that for a given beam/target angle geometry (90°) the incident beam is exited of target layer with predicted energy. To minimize the thickness of the target layer, 6° geometry is preferred; so the required layer thickness will be less with coefficient 0.1. The calculated thicknesses are shown for ideal reactions in Table 1.

Table 1.　^{117}Sb and ^{90}Nb production yields via different nuclear reactions by SRIM, TALYS-1.2 and ALICE/ASH codes.

reaction	energy range/MeV	target thickness/μm	theorical yield/(MBq/μAh)
^{117}Sn(p,n)^{117}Sb	16→9	51.38	71.41
^{118}Sn(p,2n)^{117}Sb	27→15	127.9	454.73
^{119}Sn(p,3n)^{117}Sb	36→24	166	302.29
^{120}Sn(p,4n)^{117}Sb	50→37	231	193.88
^{115}Sn(α,2n)^{117}Te→^{117}Sb	35→24	13	1.96
^{117}Sn(d,2n)^{117}Sb	18→13	26.6	25.57
^{90}Zr(p,n)^{90}Nb	19→8	85.7	613.7
^{91}Zr(p,2n)^{90}Nb	30→17	153.6	860.99
^{92}Zr(p,3n)^{90}Nb	40→27	195.5	677.84
^{89}Y(α,3n)^{90}Nb	45→35	18.56	77.82

2.5   Calculation of theoretical yield

To enhance of the projectile energy, beam current and time of bombardment increases the production yield. The production yield can be calculated by Eq. (4).

$$Y = \frac{N_L H}{M} I (1 - e^{-\lambda t}) \int_{E_1}^{E_2} \left(\frac{dE}{d(\rho x)} \right)^{-1} \sigma(E) dE, \quad (4)$$

where Y is the activity (in Bq) of the product, N_L is the Avogadro number, H is the isotope abundance of the target nuclide, M is the mass number of the target element, $\sigma(E)$ is the cross section at energy E, I is the projectile current, $dE/d(\rho x)$ is the stopping power, λ is the decay constant of the product and t is the time of irradiation [30]. The production yields of ^{117}Sb and ^{90}Nb via different reactions were calculated using the Simpson numerical integral as of Eq. (4) (Table 1).

3   Results

In the calculations of the hybrid and GDH model, the code ALICE/ASH was used (Figs. 1–5).

This code can be applied for the calculation of excitation functions, energy and angular distribution of secondary particles in nuclear reactions induced by nucleons and nuclei with energy up to 300 MeV. The generalized superfluid [31] has been applied for nuclear level density calculations in the ALICE/ASH code. The ALICE-91 and ALICE/ASH codes use the initial exciton number as $n_0 = 3$. But in these models the different alpha, deuteron and proton exciton numbers are used in the pre-equilibrium GDH model calculations. In details, the other code model parameters can be found in reference [14]. In ALICE/ASH code, the hybrid and geometry dependent hybrid model (GDH) for pre-compound emissions and the Weisskopf–Ewing model for compound reactions are selected.

Although there are some discrepancies between the calculations and the experimental data, in generally, the new evaluated hybrid and the GDH pre-equilibrium model calculations (with ALICE/ASH) are very close to the experimental data in Figs. 1, 4 and 5. In addition, the GDH and hybrid model calculations are close to each other, generally. Indeed, calculated emission cross sections with GDH and hybrid model by using ALICE/ASH code show the best agreement with the experimental data for ^{89}Y$(\alpha,3n)^{90}$Nb reaction in Fig. 5. Moreover, these cross sections are in agreement with the experimental data for ^{91}Zr(p,2n)^{90}Nb nuclei except for the (p,2n)

reaction in which the experimental data have followed above theoretical calculations in Fig. 4(b).

The reason is that the new developed pre-equilibrium reaction mechanism ALICE/ASH includes angular momentum conversion. Not only it gives us more information for new nuclear reaction research, but also it lets us calculate cross sections up to many hundreds MeV energy level. In fact, when taking the pairing energy and the mass shell correction into consideration, the experimental values are in better agreement with the theoretical results [19]. In conclusion all figures show that, although a few calculated data follow the experimental ones from above or below as parallel, generally all the compared data are in agreement with each other.

3.1   Cyclotron production of ^{117}Sb

3.1.1 ^{117}Sn(p,n)^{117}Sb reaction

The excitation functions of the proton-induced reaction on ^{117}Sn were determined by ALICE/91, ALICE/ASH and TALYS-1.2 codes (Fig. 1). The evaluation of the results of the calculations showed that the best range of energy that favors the reaction is from 16 to 9 MeV. According to the calculations from SRIM code the required target thickness should be 51.38 μm. The separation of isotope impurities is not possible by chemical methods, so this reaction is non carrier free for ^{117}Sb production. For this reaction, three cross-section measurements exist in the literature. Experimental data reported by Blaser et al. [32], Lovchikova et al. [33] and Batij et al. [34], for the energies less than 10 MeV, whereas higher energy range is required to find the maximum excitation function of the ^{117}Sn(p,n)^{117}Sb reaction.

3.1.2   Other reactions

Theoretical antimony production cross sections
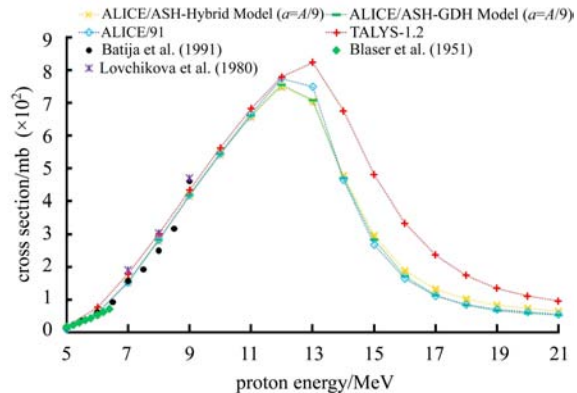
Fig. 1.   (color online) Excitation function of ^{117}Sn(p,n)^{117}Sb reaction by ALICE/91, ALICE/ASH (GDH Model & Hybrid Model) and TALYS-1.2 codes and experimental data.

have been also illustrated for ^{118}Sn(p,2n)^{117}Sb, ^{119}Sn(p,2n)^{117}Sb, ^{120}Sn(p,3n)^{117}Sb, ^{117}Sn(d,2n)^{117}Sb and ^{115}Sn(α,2n)^{117}Te→^{117}Sb in Figs. 2, 3. There have not been of any experimental data for these reactions in the literature, therefore only theoretical calculations have been shown in Figs. 2, 3. It seems that (p,2n) and (d,2n) cross section scales are higher than the others in the energy range 10–40 MeV.
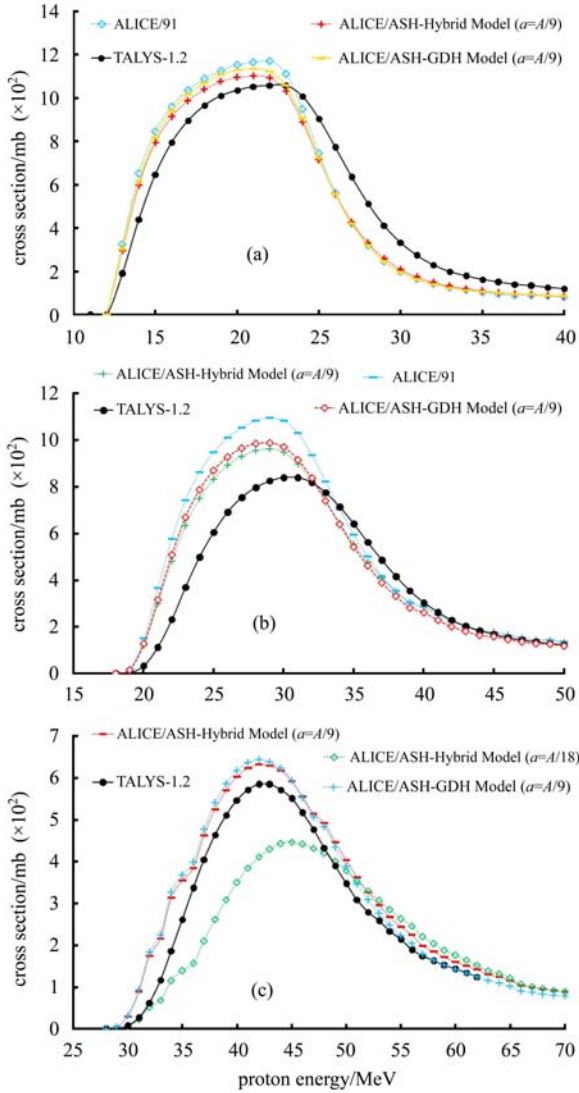
Fig. 2. (color online) Excitation function of ^{118}Sn(p,2n)^{117}Sb (a), ^{119}Sn(p,2n)^{117}Sb (b), ^{120}Sn(p,3n)^{117}Sb (c) reactions by ALICE/91, ALICE/ASH (GDH Model & Hybrid Model) and TALYS-1.2 codes. No experimental data are reported in literature.

3.2 Cyclotron production of ^{90}Nb

3.2.1 Excitation function of ^{90}Zr(p,n)^{90}Nb reaction

Figure 4(a) shows a comparison between calculated cross section of ^{90}Zr(p,n)^{90}Nb reaction from ALICE/91, ALICE-ASH and TALYS-1.2 codes, and the
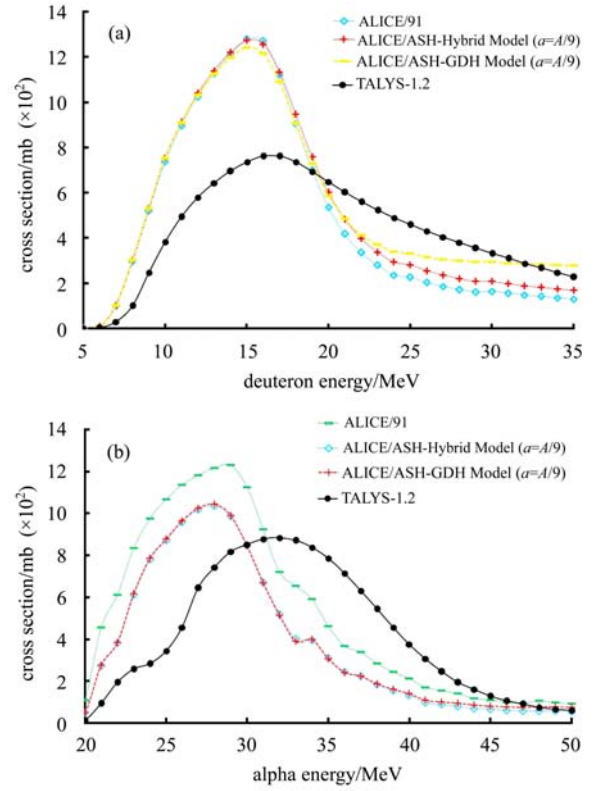
Fig. 3. (color online) Excitation function of ^{117}Sn(d,2n)^{117}Sb (a), ^{115}Sn(α,2n)^{117}Te→ ^{117}Sb (b) reactions by ALICE/91, ALICE/ ASH (GDH Model & Hybrid Model) and TALYS-1.2 codes. No experimental data are reported in literature.

experimental data reported by Levkovskij [35] and Busse et al. [9]. There is a relatively good agreement between the experimental data by Busse et al. and the prediction of the excitation function made by TALYS-1.2 code. The evaluation of the acquired data showed that the best range of the energy is 19 to 8 MeV. According to SRIM code the required target thickness should be 85.7 μm.

3.2.2 Excitation function of ^{91}Zr(p,2n)^{90}Nb reaction

The ^{91}Zr(p,2n)^{90}Nb reaction is used to produce ^{90}Nb. Fig. 4(b) shows a comparison between the calculated cross sections with TALYS-1.2, ALICE/ASH and ALICE/91 codes and experimental cross sections by Levkovskij [35]. The best range of incident energy was assumed 30 to 17 MeV; and according to TALYS-1.2 code the maximum cross section is 717.71 mb at E_{p}=22 MeV. Recommended thickness of ^{91}Zr as a target is 153.6 μm.

3.2.3 Excitation function of ^{92}Zr(p,3n)^{90}Nb reaction

According to ALICE/91, ALICE/ASH and TALYS-1.2 codes, beneficial energy range of the proton particle to produce ^{90}Nb from ^{92}Zr target is 40 to

27 MeV. The maximum cross section by TALYS-1.2 code is 484.6 mb (E_p=33 MeV). The results of nuclear model calculations by the three codes with the measurement by Levkovskij are shown in Fig. 4(c). The experimental excitation functions were obtained for energies less than 30 MeV and as shown in Fig. 4(c), the maximum cross section is located at the 33 MeV, thus nuclear model calculations can play an important role to find the maximum excitation function of ^{92}Zr(p,3n)^{90}Nb reaction.
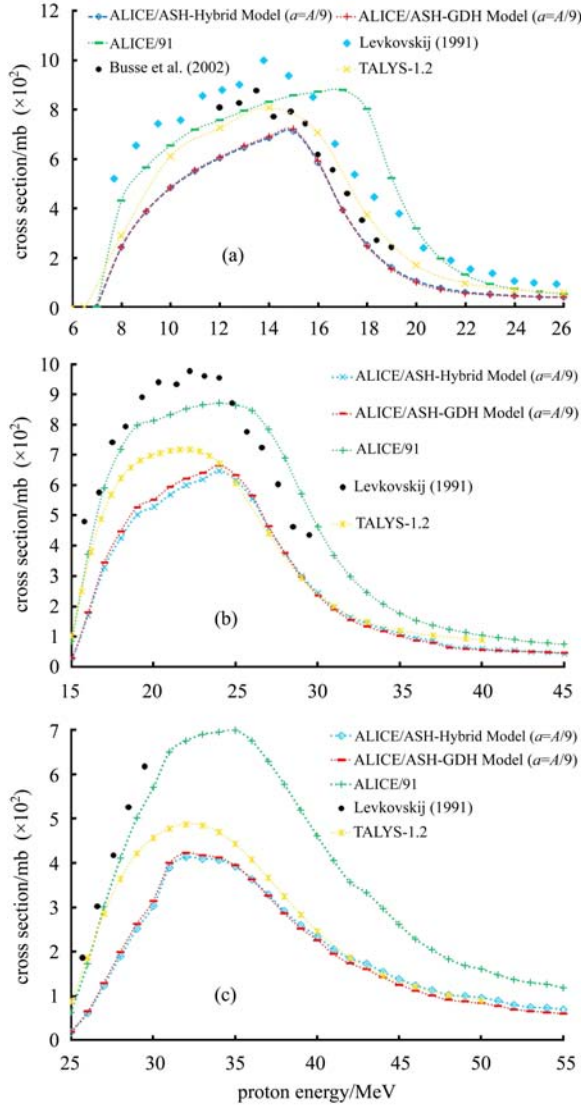
Fig. 4. (color online) Excitation function of ^{90}Zr(p,n)^{90}Nb (a), ^{91}Zr(p,2n)^{90}Nb (b), ^{92}Zr(p,3n)^{90}Nb (c) reactions by ALICE/91, ALICE/ASH (GDH Model & Hybrid Model) and TALYS-1.2 codes and experimental data.

3.2.4 Excitation function of ^{89}Y(α,3n)^{90}Nb reaction

Using ^{89}Y(α,3n)^{90}Nb reaction to produce ^{90}Nb, the best range of incident energy was assumed 45 to 35 MeV. The maximum cross section by TALYS-1.2 code is 867.906 mb (E_α=42 MeV) (Fig. 5). The theoretical thick target yield is 77.82 MBq/μAh. For this reaction, two cross-section measurements exist in the literature. Singh et al. [36] and Levkovskij [35] reported experimental data of this reaction between 46.8–28.1 MeV and 46.1–27.9 MeV, respectively. ALICE/ASH code agrees well with the measured data from Singh et al. up to 47 MeV. Also, the results of TALYS-1.2 and ALICE/91 codes are good agreement with the measured data from Levkovskij.
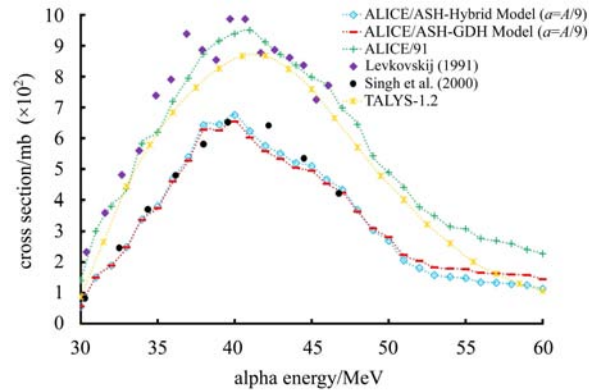
Fig. 5. (color online) Excitation function of ^{89}Y(α,3n)^{90}Nb reaction by ALICE/91, ALICE/ASH (GDH Model & Hybrid Model) and TALYS-1.2 codes and experimental data.

4 Conclusion

Cross-section data for the production of medically important radionuclides ^{117}Sb and ^{90}Nb via the proton, deuteron and alpha induced reactions on enriched tin, yttrium and zirconium isotopes were evaluated. The nuclear model codes, ALICE/91, ALICE/ASH and TALYS-1.2, were used for consistency checks of the experimental data.

By some adjustments in the nuclear model parameters, generally good agreement was achieved between calculated and measured excitation functions, both for proton and deuteron induced reactions. The recommended data should be useful for optimization of various routes for the production of ^{117}Sb and ^{90}Nb at cyclotrons. The production of ^{117}Sb and ^{90}Nb can be achieved by ^{117}Sn(p,n)^{117}Sb and ^{90}Zr(p,n)^{90}Nb ideal reactions for low energy cyclotrons.

References

1 Rösch F, Herzog H, Stolz B et al. Eur. J. Nucl. Med., 1999, **26**: 358–366

2 Thisgaard H, Jensen M. Med. Phys., 2008, **35**: 3839–3846

3 Thisgaard H. Accelerator Based Production of Auger-Electron Emitting Isotopes for Radionuclide Therapy. PhD Thesis. Risø-PhD-42(EN), 2008

4 Bishayee A, Rao D V, Howell R W. Acta Oncology, 2000, **39**: 713–717

5 Kassis A, J. Nucl. Med., 2003, **44**: 1479–1481

6 Kassis A, Adelstein S J, J. Nucl. Med., 2005, **46**: 4S–12S

7 Kassis A I, Semin. J. Nucl. Med., 2008, **38**: 358-366

8 Maiti M, Lahiri S, J. Radioanal. Nucl. Chem., 2010, **283**:637–640

9 Busse S, Rösch F, Qaim S M, Radiochim. Acta., 2000, **90**: 1–5

10 Qaim S M. Radiochim. Acta., 2001, **89**: 189-355

11 Stocklin G, Qaim S M, Rosch F. Radiochim. Acta., 1995, **249**: 70–71

12 Blann M. ALICE-91-RSIC CODE PACKAGE PSR-146, 1991 USA

13 Konobeyev A Yu, Korovin, Yu A, Pereslavtsev P E. Code ALICE/ASH for Calculation of Excitation Functions, Energy and Angular Distributions of Emitted Particles in Nuclear Reactions. Report of the Obninsk Institute of Nuclear Power Engineering, 1997

14 Broeders C H M, Konobeyev A Yu, Korovin Yu A. ALICE/ASH–Pre-Compound and Evaporation Model Code System for Calculation of Excitation Functions, Energy and Angular Distributions of Emitted Particles in Nuclear Reactions at Intermediate Energies. Forschungszentrum Karlsruhe GmbH, Karlsruhe, Report FZKA, 2006 <http://bibliothek.fzk.de/zb/berichte/FZKA7183.pdf>

15 Koning A J, Hilaire S, Duijvestijn M. TALYS-1.2 A Nuclear Reaction Program, User Manual. NRG, Netherlands, 2009

16 Sato K, Iwamoto A, Harada K. Phys. Rev. C, 1983, **28**: 1527–1537

17 Blann M, Vonach H K. Phys. Rev. C, 1983, **28**: 1475–1492

18 Kaplan A, Aydin A. PRAMANA J. Phys., 2009, **72**: 343–353.

19 Büyükuslu H, Kaplan A, Tel E, Aydin A, Yıldırım G, Bölükdemir M H. Ann. Nucl. Energy, 2010, **37**: 534–539

20 Raynal J. Notes on ECIS–94. CEA Saclay Report No. CEA-N-2772, 1994

21 Koning A J, Delaroche J P. Nucl. Phys. A, 2003, **713**: 231–310

22 Watanabe S. Nucl. Phys., 1958, **8**: 484–492

23 Belgya T, Bersillon O, Capote R, Fukahori T, Zhigang G, Goriely S et al. Handbook for Calculations of Nuclear Reaction Data, Reference Input Parameter Library-2, Tech. Rep. IAEA-TECDOC-1506. IAEA, Vienna, Austria, 2006, 1–159

24 Moldauer P A. Nucl. Phys. A, 1980, **344**: 185–195

25 Koning A J, Duijvestijn M C. Nucl. Phys. A, 2004, **744**: 15–76

26 Kalbach C. Phys. Rev. C, 2005, **71**: 034606

27 Dilg W, Schantl W, Vonach H, Uhl M. Phys. A, 1973, **217**: 269–298

28 Aslam M N, Sudár S, Hussain M, Malik A A, Shah H A, Qaim S M. Appl. Radiat. Isot., 2010, **68**: 1760–1773

29 Ziegler J F, Biersack J P, Littmark U. SRIM Code. USA, 2006

30 Sadeghi M, Zali A, Zeinali B. Appl. Radiat. Isot., 2009, **67**:1393–1396

31 Ignatyuk A V, Istekov K K, Smirenkin G N. Yad. Fiz., 1979, **29**: 875–883

32 Blaser P, Boehm F, Marmier P, Peaslee D. Helvetica Phys. Acta, 1951, **24:** 3–5

33 Lovchikova G N, Salnikov O A, Simakov S P et al. Sov. J. Nucl. Phys., 1980, **31**: 1–5

34 Batij V G, Skakun E A. Nucl. Struct C, 1991, **91**: 248

35 Levkovskij V N. Activation Cross Section Nuclides of Average Masses (A=40–100) by Protons and Alpha-Particles with Average Energies (E=10–50 MeV). Moscow, 1991

36 Singh N L, Gadkari M S, Chintalapudi S N. Phys. Scripta, 2000, **61**: 550–554